View metadata, citation and similar papers at core.ac.uk
brought to you by CORE
provided by Loughborough University Institutional Repository

A Bifurcation Analysis of an Open Loop Internal Combustion Engine

Abstract

The process of engine mapping in the automotive industry identifies steady-state engine responses by running an engine at a given operating point (speed and load) until its output has settled. While the time simulating this process with a computational model for one set of parameters is relatively short, the cumulative time to map all possible combinations becomes computationally inefficient. This work presents an alternative method for mapping out the steady-state response of an engine in simulation by applying bifurcation theory. The bifurcation approach used in this work allows the engine's steady-state response to be traced through the model's state-parameter space under the simultaneous variation of one or more model parameters. To demonstrate this approach, a bifurcation analysis of a simplified nonlinear engine model is presented. Using "throttle demand" and "desired load torque signal", the engine's dynamic response is classified into distinct regions bounded by bifurcation points. These bifurcations are shown to correspond to key physical properties of the open-loop system: fold bifurcations correspond to the minimum throttle angle required for a steady-state engine response; Hopf bifurcations bound a region where self-sustaining oscillations occur. The techniques used in this case study demonstrate the efficiency a bifurcation approach has at highlighting different regions of dynamic behavior in the engine's state-parameter space. Such an approach could speed up the mapping process and enhance the automotive engineer's understanding of an engine's underlying dynamic behavior. The information obtained from the bifurcation analysis could also be used to inform the design of future engine control strategies.

Introduction

Computer models of nonlinear automotive systems are conventionally analyzed using time-domain simulations. Using a mathematical model of the engine and conducting desktop-based analysis is extremely valuable to engineers, however simulations are not without limitations. A traditional time-domain analysis gathers information by running a time history simulation for a set of input parameters. Once the simulation has settled, the inputs can be mapped to a steady-state engine response. While a simulation for a single set of input parameters and initial conditions is relatively short, a full analysis requires multiple simulations for many combinations of input parameters and initial states. The cumulative time needed to fully map an engine with this approach alone makes the process a computationally-expensive task. When the interest of a time-domain analysis for engine mapping is the steady state response, time is wasted calculating transient behavior that occurs prior to reaching steady state. Another limitation of conventional time history simulations is that it can be difficult to identify the location of unstable equilibria. In practice, unstable equilibria often separate regions of the state space, so knowledge of their location can allow engineers to identify regions in their model's state space where similar initial conditions may have quite different steady-state responses.

A wide range of complementary approaches to time history simulations have been proposed in the literature to investigate the dynamic behavior of engine models. Recurrence plots have been used to provide insight into the deterministic nature of engine parameters injection impulse width and engine angular speed [1]. Recurrence plot and recurrence quantification analysis were used to investigate the dynamics associated with cycle-to-cycle variations in a diesel engine [2]. Multi-level sub structuring procedures were applied to study the periodic steady-state response of large engine models in a computationally-efficient way [3]. 0-1 testing, which is a relatively simple method of determining whether the system is regular or chaotic, was applied to study behavior of the combustion process [4]. Such approaches serve to enhance the automotive engineer's toolbox of analysis techniques, allowing specific information from a dynamic model to be obtained efficiently.

Another complementary approach to the analysis of nonlinear dynamic systems is to conduct a bifurcation analysis of the engine model. Bifurcation theory is the study of qualitative changes in the equilibria of a system of differential equations. The point at which the system undergoes a qualitative change is a "bifurcation point", or simply "bifurcation". By representing the dynamics of the non-linear engine as a series of first-order differential equations, a bifurcation study determines the position and nature of equilibria as one or more parameters are simultaneously varied. This is achieved with a method known as numerical continuation: starting from a known steady-state response, the continuation algorithm traces branches of equilibria as a parameter is varied, and identifies changes in these equilibria as bifurcation points. The results from a numerical continuation run can be displayed visually on a bifurcation diagram. These bifurcation diagrams provide a useful and efficient source of information that illustrates the long-term behavior of the nonlinear dynamic system in the state-parameter space. For further information on bifurcation theory, see [5,6].

Bifurcation analysis methods have been used in a variety of engineering disciplines, including aeronautical and automotive engineering: in [7], a bifurcation approach was used to determine safe and unsafe operating regions of an aircraft maneuvering on the ground, highlighting key parameter values that produced undesirable responses; in [8], bifurcations were discovered that corresponded to dangerous situations (such as the loss of cornering stability).

The aim of this paper is to demonstrate a bifurcation analysis of a simple open-loop engine model to demonstrate the benefits of applying numerical bifurcation theory to engine modeling. The efficiency of mapping the state parameter space with branches is shown to be advantageous over time history simulations alone, and physical properties of the system can be linked to bifurcation points.

To conduct the bifurcation analysis in this work, the numerical continuation code AUTO [9,10,11] integrated into MATLAB via the dynamical systems toolbox [12] is used. An overview of the mathematical engine model is provided, followed by an initial bifurcation analysis of the engine's dynamics for different throttle and desired load torque settings. The initial findings present key areas of the state parameter space which are then explored in a further analysis. After providing an overview of the system's bifurcation behavior, the sensitivity of this behavior to changes in additional parameters is determined. Finally, the key findings are summarized and recommendations for future work are outlined.

Mathematical Model

This work uses a mean value model based on work by Guzella and Onder [13]. The spark ignition engine model is governed by three coupled first order nonlinear differential equations. Equations (1),(2) & (3) represent the dynamics associated with the intake manifold P_m, engine speed $_e$, and torque, T_l, respectively. The model contains several parameters: R is the gas constant of air; is the temperature of air in manifold; is the volume of intake manifold; $\Theta_e$is the engine inertia; is a time constant. The system has two input parameters: "throttle demand", which ranges from fully closed, 0, to fully open, 1;"desired load torque", u_l, which is measured in Nm.

(1)

(2)

(3)

The first differential equation represents the dynamics that occur as the mass flow enters, m_α, and exits, m_β, the manifold. The throttle mass flow equation (4) uses a tanh approximation to ensure that the resulting model is smooth (a condition required for the bifurcation analysis):

(4)

Here, a, b, c and d are numerically fitted parameters that are chosen to approximate the piecewise throttle model from [13]. p_a and ϑ_a are ambient pressure and temperature respectively.

The throttle area, $_\alpha$, depends on the input as shown in equation (5):

(5)

Here; is the diameter of the throttle; is the offset; is the leakage area.

(6)

Here: is the compression volume at top dead centre; $_d$is the displacement volume; is the exhaust-manifold pressure; κ is isentropic exponent air; γ_0, $\gamma_1$and are gear ratios; λ and are the coefficient and the stoichiometric values for air to fuel ratio.

The dynamics associated with the engine speed (2) is the scaled difference between torque generation (7) and load torque (3)

(7)

The terms η_0, are Willans parameters, which are simplifications of the engine's characteristics, while represents Enthalpy.

The final differential equation represents load torque, and equals u_l after a short delay. Here u_l is chosen to represent the sum of resistance forces that are applied to the engine such as air and rolling resistance. The numerical values for all parameters used in this work are summarized in table 1.

Table 1. Summary table of all parameters and numerical values used.

Parameter	Symbol	Value	Unit
Gas constant air		287	
Temperature of air in manifold		340	
Volume of intake manifold			
Engine Inertia		0.2	
Time constant		0.02	
Ambient Pressure			
Ambient temperature		298	
Fitted parameter 1		-0.3540	[-]
Fitted parameter 2		10	[-]
Fitted parameter 3		7	[-]
Fitted parameter 4		0.3531	[-]
Throttle diameter			
Angle offset		7.9	
Leakage area			
Compression volume at top dead centre			
Displacement			
Back pressure exhaust manifold			
Isentropic exponent air		1.35	[-]
Air to fuel ratio coefficient		1	[-]
Stoichiometric air to fuel ratio		14.7	[-]
Coefficient 1		0.45	[-]
Coefficient 1			
Coefficient 1			
Willans parameter 1		0.16	
Willans parameter 2			
Enthalpy		42390000	
Willans parameter 3		15.6	
Willans parameter 4			

One-Parameter Bifurcation Analysis

This section presents a bifurcation analysis of the previously introduced engine model, to demonstrate the results that can be obtained from a bifurcation approach.

For initial analysis, a case is chosen to represent an automobile on an incline; u_l is fixed to 100Nm. As only one of the inputs, u_α, is varied, the results are presented in the form of a one-parameter bifurcation diagram. Note that the state space is three dimensional, however for readability the results are displayed graphically in 2 dimensions, with each state being shown as a function of the continuation parameter . As $T_l(t) = u_l$ for $t \to \infty$, only the states p_m and ω_e are shown.

Figure 1 shows the engine's steady-state response as a function of throttle angle, in the form of a bifurcation diagram. Figure 1(a) shows the manifold pressure of the system as a function of while figure 1(b) shows the systems engine speed as a function of $_\alpha$. Here and throughout the paper, blue solid lines indicate dynamically-attracting equilibria; red dashed lines indicate dynamically-repelling equilibria. The black circle indicates a fold bifurcation and is the point at which the branches change from repelling to attracting. For this single desired torque single, the state parameter space has been mapped efficiently across the entire $u_\alpha \in [0\ 1]$. The system undergoes a fold bifurcation at $u_\alpha = 0.0916$: for throttle settings below this value, the engine cannot sustain a non-zero steady-state engine response; for throttle settings above this value, equilibria exist so the engine can reach a non-zero steady-state. Therefore, the fold bifurcation is the system's minimum throttle demand.

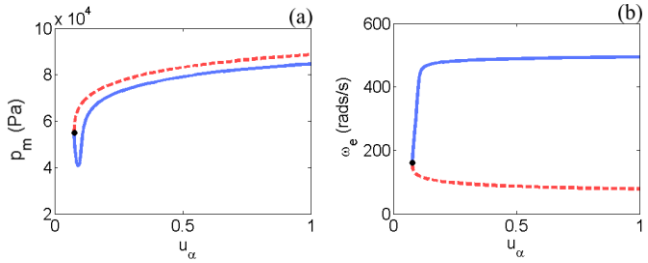

Figure 1. One-parameter bifurcation diagram showing the response of (a) manifold pressure and (b) engine speed for a fixed load torque $u_l = 100$Nm. Blue solid lines indicate dynamically-attracting equilibria; red dashed lines indicate dynamically-repelling equilibria. A black circle indicates the location of a fold bifurcation.

The bifurcation diagram enables the trajectory of any initial condition (i.e. initial value at t=0 for manifold pressure and engine speed) in the state parameter space to be inferred. Attracting equilibria cause nearby states to tend towards them over time; repelling equilibria cause nearby states to move away over time. The transient trajectory for any initial condition can therefore be predicted based on the location of the attracting and repelling equilibrium branches.

Figure 2 provides some examples of this predictive capability. With a throttle demand of $u_\alpha = 0.8$, the outcome of a time history simulation with initial condition A ($\omega_e = 300$) will produce a steady-state response, as the trajectory tends away from the repelling branch and towards the attracting branch. Similarly, if the initial condition of engine speed is raised as in example B ($\omega_e = 550$), the bifurcation diagram shows that a steady state response will be achieved, as the trajectory will tend towards the attracting branch. However, if the initial condition of engine speed is lowered so it is below the repelling branch as in example C ($\omega_e = 60$), the bifurcation diagram can be used to infer that the engine speed will be repelled towards 0. For completeness, for simulation D ($\omega_e = 400$), which has a throttle demand of $u_\alpha = 0.05$, there is no equilibria and therefore the trajectory heads towards zero engine speed. Here, the role of repelling equilibria is clear in that they create a boundary between initial conditions that do or do not lead to a non-zero steady-state engine response.

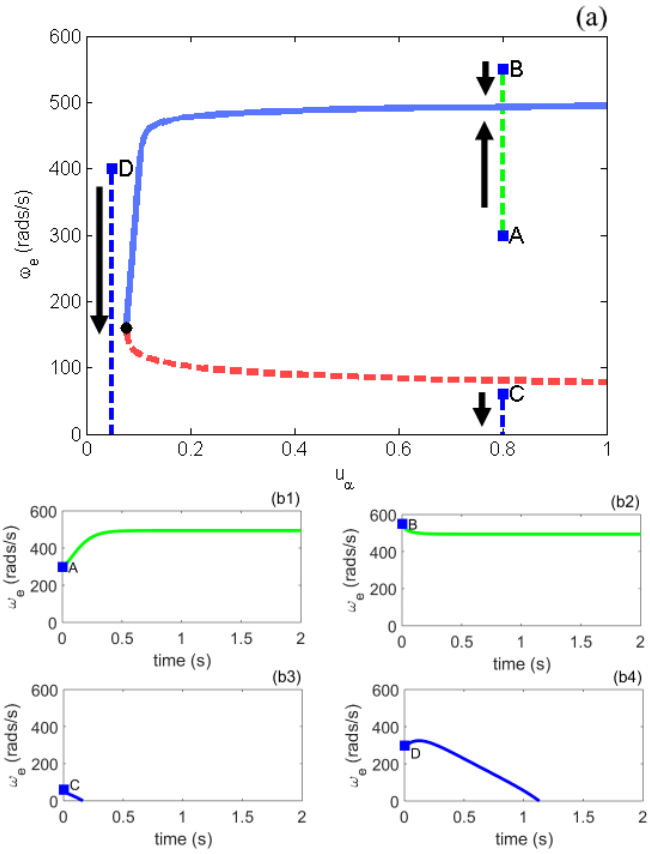

Figure 2. Four example initial conditions (A,B,C,D), are shown on the bifurcation diagram and as a time history. Green trajectories arrive at the stable branch while blue trajectories do not reach this steady state response.

To see how the system behaves in another area of the state-parameter space, a different load torque can be chosen. For a second analysis, the case of an automobile cruising is chosen, so u_l is fixed to 10Nm.

Figure 3 shows a bifurcation diagram for fixed 10Nm. A Hopf bifurcation, represented here and throughout by a purple star, is observed at $u_a = 0.0147$. A Hopf bifurcation indicates the point at which a periodic response arises, in the form of a limit cycle oscillation. The amplitudes of these limit cycle oscillations, shown in green, grow from the Hopf bifurcation as the throttle demand decreases. This Hopf bifurcation is a key point in the state parameter space, as throttle demands below $u_a = 0.0147$ will result in self-sustaining periodic responses, while throttle demands above u_a result in attracting equilibrium behavior.

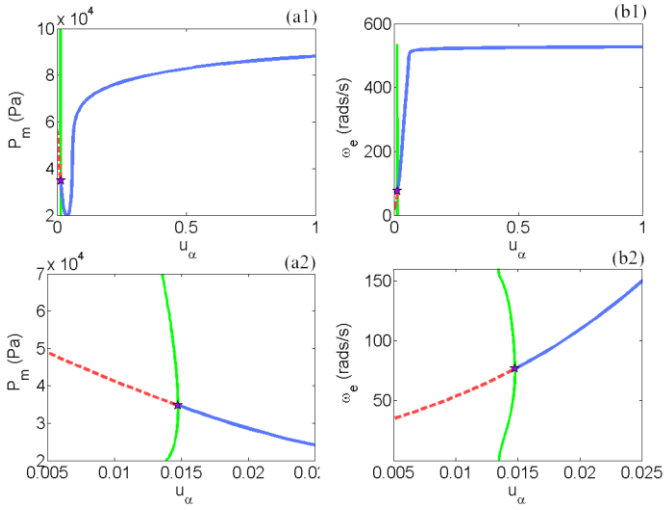

Figure 3. One-parameter bifurcation diagram showing the response of (a1) manifold pressure and (b1) engine speed (with zoomed view (a2) and (b2) below) for $u_l = 10$Nm. A purple star indicates the location of a Hopf bifurcation.

Figure 4(a) contains a time history simulation for $u_a < 0.0147$. It shows that the system exhibits an oscillatory response, and that the amplitude of these oscillations reaches a constant value after an initial transient period of about 20 seconds. Figure 4(b) shows a time-history simulation for $u_a > 0.0147$, which shows that the system is able to reach a steady-state response. The behavior in figure 4 arises because of the presence of a supercritical Hopf bifurcation.

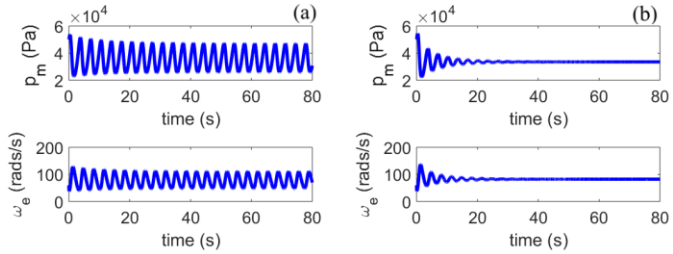

Figure 4. A time history simulation for $u_a < 0.0147$ (a) showing a periodic response and a time history simulation for $u_a > 0.0147$ (b) showing the solution decaying to steady state, as could be inferred from the bifurcation diagram.

The Hopf bifurcation and behavior in figures 3 & 4 represent the physical properties that occur in the engine as the throttle angle transitions from closed to open. For low throttle positions, the throttle is open to the point at which there is enough air to increase the engine's speed for a short duration. As the engine speeds up, its momentum causes it to overshoot the speed that could be maintained with the current flow of air through the throttle. This causes there to be a lack of airflow at the peak engine speed, which means that the engine begins to slow down. As the engine decelerates, the airflow through the throttle becomes sufficient to increase the engine's speed once more, and the cycle repeats itself. This behavior is shown by the out of phase response in figure 4. As throttle is increased past the Hopf bifurcation point, the engine receives enough airflow to maintain a steady engine speed.

Two-Parameter Bifurcation Analysis

To understand where each bifurcation exists throughout system, the evolution of both the fold and the Hopf bifurcations can be traced numerically as throttle position and load torque are varied simultaneously – this process is referred to as a two-parameter continuation run. In a two-parameter continuation run, the fold and Hopf bifurcations observed in figures 1 and 3 are traced as throttle angle and load torque are varied simultaneously. The results are presented in a two-parameter continuation diagram, as shown in figure 5. This shows the location of these two bifurcations in terms of throttle position and torque value. The purple dashed purple line indicates the loci of Hopf bifurcations and the black line indicates the loci of fold bifurcations. For higher values of load torque, a single fold bifurcation occurs. This indicates that the one-parameter bifurcation diagram will be similar to that shown in figure 1. For very low torques, only a Hopf bifurcation is present, so the behavior will be similar to that described in figure 3.

The grayed-out section represents the region of the parameter space where no attracting equilibria exist: running any time history simulation at an operating with parameter values in this region will drive the engine speed towards zero as seen in figure 2(b2). Such observed behavior in this region is independent of the choice of initial condition – a result that highlights the analysis power offered by performing a bifurcation analysis. To explain how this shaded region can be inferred, the behavior that occurs between the previously identified low (figure 3) and high (figure 1) load torque cases will be examined.

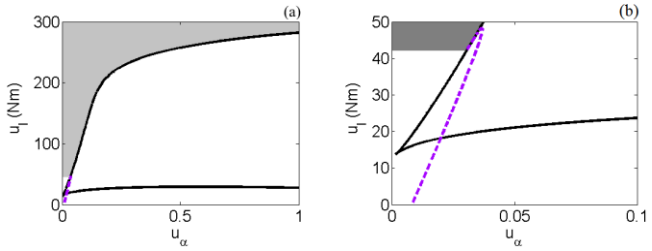

Figure 5. Two-parameter continuation of the fold and Hopf bifurcation points for (a) $u_\alpha \in [0\ 1]$ and a zoomed view (b) of the point where both bifurcations collide: black lines indicate loci of fold bifurcations; purple dashed lines show loci of Hopf bifurcations. The shaded region indicates parameter values that do not lead to a steady-state engine response.

Between the two load cases considered in the one-parameter bifurcation analysis section, where the curves overlap and turn back on themselves, multiple fold and Hopf bifurcations may be present depending on the exact value of load torque chosen. The grayed out sections shows operating points in which no equilibria exist. For other regions, both attracting and repelling equilibria exist in the parameter space and therefore running a time history simulation at these operating points means the behavior is dependent upon initial conditions. An added conclusion of a two-parameter continuation is that the system peak load torque is also found in a two-parameter continuation, as for a throttle completely open the maximum torque demand that can be met by the engine is given by the peak of the fold curve, which occurs around 282Nm.

To explore exactly what behavior exists in the parameter region where the two bifurcation curves overlap, further one-parameter bifurcation diagrams can be created at specific torque values. The five horizontal lines in figure 6 indicate load torque values that will be considered in subsequent one-parameter bifurcation diagrams. Each line represents torque values that have different bifurcation behavior in their state parameter space. Case v was shown in figure 5, and is representative of the dynamics from $u_l = 0$ until the system undergoes what is called a cusp bifurcation – a point at which two fold bifurcations meet.

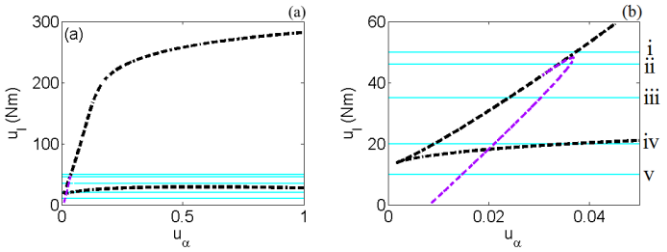

Figure 6. Two parameter bifurcation diagram (a) with zoom (b) showing 5 (i-v) key desired torque signals that will be taken forward for further analysis.

Figure 7 shows the one-parameter bifurcation diagram that corresponds to case iv in figure 6, just after the system has passed the cusp point. Here, two fold bifurcations are observed along with a Hopf bifurcation. The size of the amplitudes from the Hopf point rapidly grow until they collide with the branch of repelling equilibria to create a homoclinic orbit. To the left of this homoclinic orbit, no periodic behavior is present and only repelling equilibria exist. Time history simulations in this region would show the trajectories heading towards a zero engine speed: for very low throttle angles, not enough air can get through so the engine speed is driven towards zero. The homoclinic orbit and Hopf bifurcation bound the region in which periodic oscillations occur.

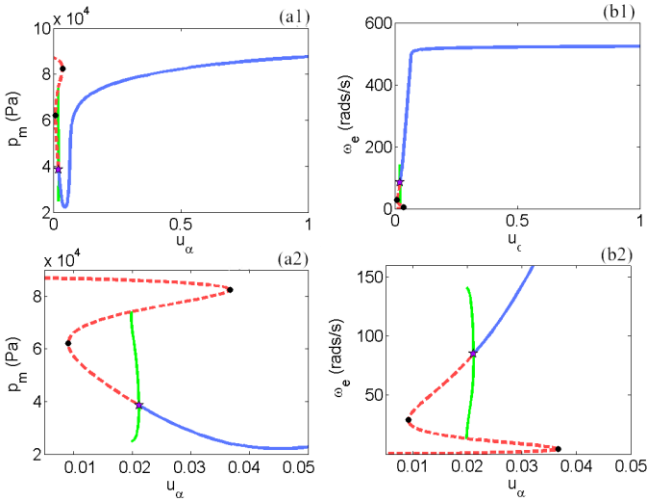

Figure 7. One-parameter bifurcation diagram showing the response of (a1) manifold pressure and (b1) engine speed (with zoomed view (a2) and (b2) below) for $u_l = 20$Nm.

As torque is increased further, one of the two fold bifurcations moves further from the other until it leaves the range of physically-meaningful throttle positions. Case iii from figure 6 is shown as a one-parameter bifurcation diagram in figure 8: for this load torque value, no equilibria exist at low throttle angles.

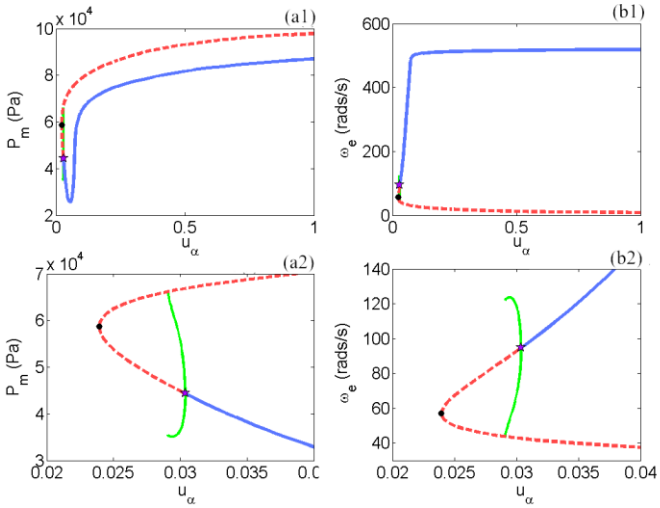

Figure 8. One-parameter bifurcation diagram showing the response of (a1) manifold pressure and (b2) engine speed (with zoomed view (a2) and (b2) below) for $u_l = 35$Nm.

As the torque is raised further still, a second Hopf bifurcation arises from a point known as a Bogdanov-Takens bifurcation. Figure 9 is the one-parameter bifurcation diagram for case ii: the periodic limit cycle is bound by two Hopf bifurcations, rather than one Hopf bifurcation and a homoclinic orbit.

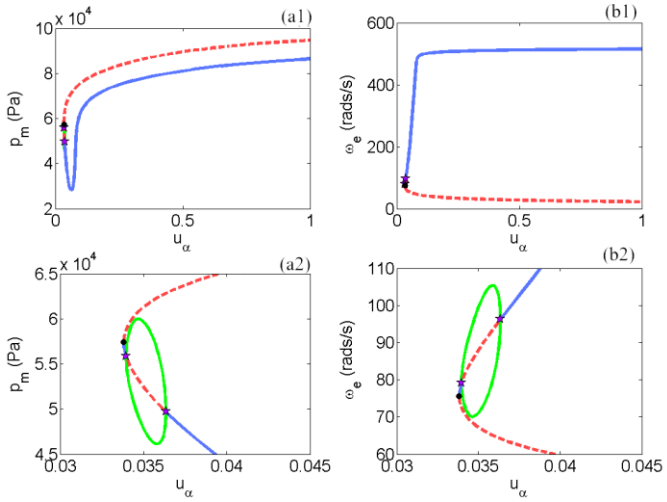

Figure 9. One-parameter bifurcation diagram showing the response of (a1) manifold pressure and (b1) engine speed (with zoomed view (a2) and (b2) below) for $u_l = 46$Nm.

As torque is increased even more, these Hopf bifurcations grow closer and closer until they collide and are destroyed. Figure 10 is the one-parameter bifurcation diagram for case i, and shows the behavior that is like that of figure 1. The qualitative description in figure 1 is relevant for torque values until the peak load torque of Nm, as the minimum throttle demand increases until it outside the physically meaning region.

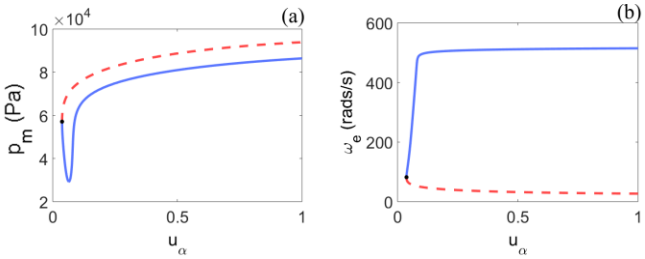

Figure 10. One-parameter bifurcation diagram showing the response of (a) manifold pressure and (b) engine speed for $u_l = 50$Nm.

It is noted in figures 8, 9 and 10 that the branch of attracting equilibria has a very similar structure: this information could be obtained, albeit in a more time consuming way, via conventional time history simulations. Detecting the changes in the branch of repelling equilibria would be much more difficult to do with traditional time history simulations alone. With traditional methods many simulations would be needed to approximate this branch. For a single u_α and u_l, time history simulations would have to be ran for many different initial conditions either side of the branch of repelling equilibria. This process would then have to be repeated for further combinations of u_α and u_l which, when pieced together, would only approximate the location of the repelling branch.

Sensitivity Analysis of the Bifurcation Diagrams

With an overview of the bifurcations present in the system's state-parameter space, a bifurcation sensitivity analysis can be conducted. Here, some of the nominal parameter values of the model are altered to determine the extent to which parameter variations could change the steady-state behavior of the system. Running the two-parameter continuations when one or more nominal parameters are changed will show how sensitive these bifurcations are to changes in certain parameters.

Air-fuel ratio λ, which in the model is assumed be fixed at the stoichiometric value $\lambda = 1$ by a controller, is likely to undergo some deviation during driving. Figure 11 shows the bifurcation sensitivity analysis for λ. Running continuations for different λ values either side of $\lambda = 1$ show no qualitative change to the bifurcation behavior. These two-parameter continuations are performed at extremely rich and lean values that far exceed any legal boundaries, to capture the insensitivity of the model to changes in λ.

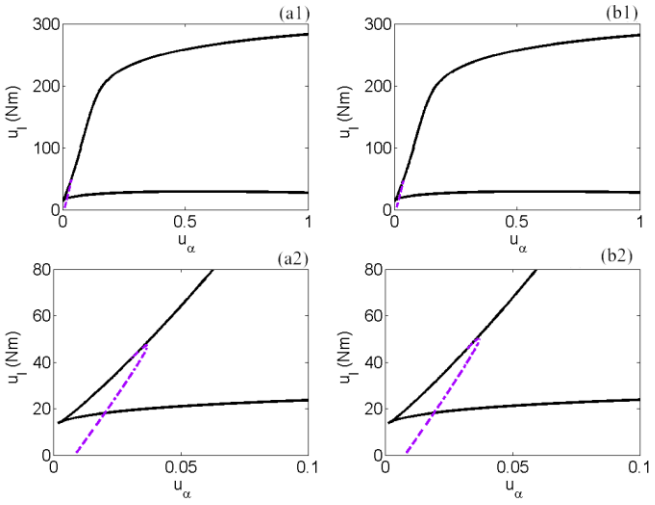

Figure 11. Two two-parameter bifurcation diagrams for (a1) =0.6, and (b1) =1.4 (with zoomed view (a1) and (b2) below).

Ambient pressure is also assumed to be fixed at $P_a = 0.98 \times 10^5$. An increase in ambient pressure as shown in figure 12 provides a crude representation of the effects of turbocharging an engine. The results show that an increase in peak load torque occurs as pressure increases to $1.5 \times P_a$ and $2 \times P_a$. Increasing the value of P_a also causes a change in the Hopf bifurcation curve: it reaches a higher torque value before turning around and colliding with the fold locus, indicating a growth in the region where periodic responses are expected. The figures also show a non-linear relationship between peak load torque and ambient pressure as an increase of a factor of 1.5 and 2 increase the peak load torque by more than these amounts.

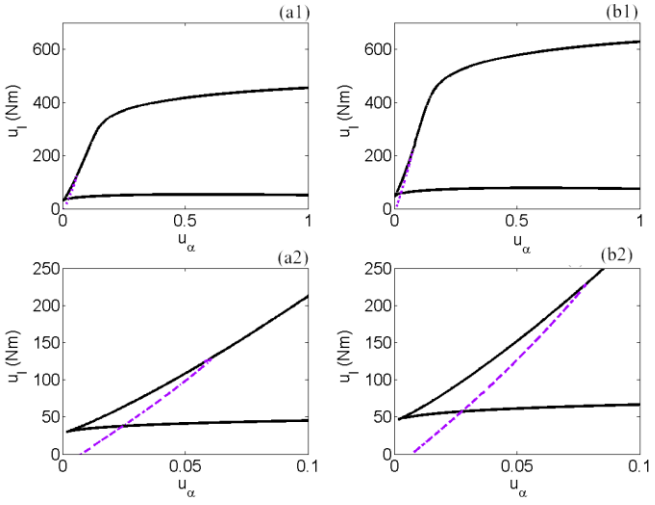

Figure 12. Two two-parameter bifurcation diagrams for (a1) ≈1.5 bar and (b1) P_a ≈2 bar (with zoomed view (a1) and (b2) below).

A decrease in ambient pressure, along with a decrease in the ambient temperature, can be used to replicate the effects of the engine operating at higher altitudes: two-parameter bifurcation diagrams for such a case is shown in figure 13. Increasing the altitude to 2000m and 5000m will replicate the engine running in extreme physical conditions. Opposite changes are observed to those shown by the previous result in figure 12: a higher altitude limits the airflow into the system, reducing the amount of torque that can be demanded at a given throttle angle; the Hopf bifurcation is reduced until it is no longer present in the physically-meaningful region. As before, the relationship is non-linear. At 5000m, the Hopf bifurcation no longer exists in the physically possible region as it has been suppressed below $u_\alpha = 0$.

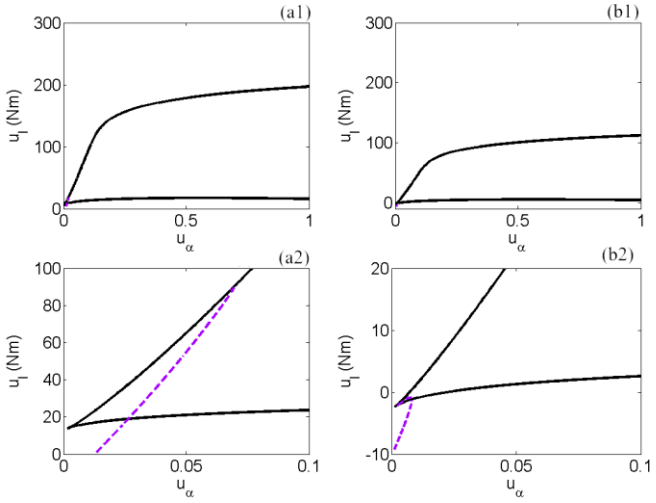

Figure 13. Two two-parameter bifurcation diagrams for an altitude of (a1) 2000m and (b1) 5000m (with zoomed view (a1) and (b2) below).

A final parameter is chosen to replicate a change that could be made in the design process: the engine inertia value is altered in figure 14, replicating an increase or decrease in the size of the flywheel. There is no qualitative change in the fold bifurcations behavior; however a smaller flywheel increases the amount of demand torque the Hopf bifurcation is present for. A larger flywheel decreases the range of Hopf bifurcation and causes the Bogdanov-Takens bifurcation to occur outside the physically-meaningful range, meaning that only one Hopf bifurcation will be observed at any single torque value.

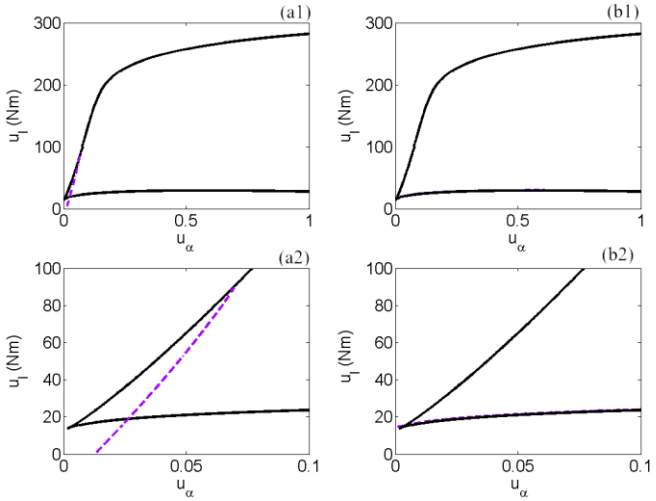

Figure 14. Two two-parameter bifurcation diagrams for (a1) , and (b1) Θ (with zoomed view (a1) and (b2) below).

The four alterations in lambda, ambient pressure, and altitude and engine inertia are a demonstration that shows how a bifurcation sensitivity analysis can quantify the effects of additional parameters that may cause a qualitative change should they deviate from their fixed value. Mechanical alterations, such as changing the size of the

flywheel, alter the location of the Hopf bifurcation. In comparison, alterations involving the airflow, such as changing altitude, disturb the location of the fold bifurcation. This demonstrates the capability that a bifurcation analysis has in determining the location of qualitatively different behavior based on a change in one or more parameters. Furthermore, a bifurcation approach has the ability to classify which type of alteration, such as mechanical, are likely modify which behavior.

Conclusions

This work demonstrates how a bifurcation analysis can be used to offer a complementary approach to analyze the dynamics of a non-linear engine model. The tool of numerical continuation offers an efficient method of mapping the state parameter space, enabling key properties of the system to be highlighted. By tracing a steady-state response across an entire parameter range, branches of dynamically-repelling and dynamically-attracting equilibria allow the user to determine the output of any time history simulation in the state-parameter space. Bifurcation points observed, such as fold and Hopf bifurcations, can provide physical boundaries to the engine's operation, such as the minimum throttle angle or peak load torque. A subsequent bifurcation sensitivity analysis highlights the parameters that may cause a qualitative change in the system's dynamics. Alterations in the parameters which relate to the mechanical and air flow properties are shown to affect the state-parameter regions in which different types of bifurcation exist – such information could help inform the design of future engine control strategies.

Future work could be conducted on a more realistic engine model, as a full bifurcation study on a more representative model could develop fundamental knowledge about how computational engine models behave. Running a similar analysis on an emissions model could prove to effective tool to analyzing the influence of control parameters on emissions output. Furthermore, knowledge of where bifurcations exist, and how they change, could aid the development of future engine control strategies, by informing engineers of where qualitative changes in the system's dynamic response will occur.

References

1. Alexa, O., C. O. Ilie, M. Marinescu, R. Vilau, and D. Grosu. "Recurrence Plot for Parameters Analysing of Internal Combustion Engine." *IOP Conference Series: Materials Science and Engineering* 95 (2015): 012121. doi:10.1088/1757-899x/95/1/012121.

2. Ding, S., Yang, L., Song, E., and Ma, X., "Investigations on In-cylinder Pressure Cycle-to-Cycle Variations in a Diesel Engine by Recurrence Analysis," SAE Technical Paper 2015-01-0875, 2015, doi:10.4271/2015-01-0875.

3. Theodosiou, C., K. Sikelis, and S. Natsiavas. "Periodic Steady State Response of Large Scale Mechanical Models with Local Nonlinearities." *International Journal of Solids and Structures*, 2009. https://doi.org/10.1016/j.ijsolstr.2009.06.007.

4. Ding, Shun Liang, En Zhe Song, Li Ping Yang, Grzegorz Litak, et al. "Analysis of Chaos in the Combustion Process of Premixed Natural Gas Engine." *Applied Thermal Engineering*, 2017. https://doi.org/10.1016/j.applthermaleng.2017.04.109.

5. Strogatz, Steven H. *Nonlinear Dynamics and Chaos: With Applications to Physics, Biology, Chemistry, and Engineering*. Boulder, CO: Westview Press, a Member of the Perseus Books Group, 2015.

6. Yuznetsov, Yuri A. *Elements of Applied Bifurcation Theory*. New York: Springer, 2004.

7. Rankin, James, Bernd Krauskopf, Mark Lowenberg, and Etienne Coetzee. "Operational Parameter Study of Aircraft Dynamics on the Ground." *Journal of Computational and Nonlinear Dynamics* 5, no. 2 (2010): 021007. doi:10.1115/1.4000797.

8. Rossa, Fabio Della, Giampiero Mastinu, and Carlo Piccardi. "Bifurcation Analysis of an Automobile Model Negotiating a Curve." *Vehicle System Dynamics* 50, no. 10 (2012): 1539-562. doi:10.1080/00423114.2012.679621.

9. Doedel, Eusebius, Herbert b. Keller, and Jean Pierre Kernevez. "numerical analysis and control of bifurcation problems (ii): bifurcation in infinite dimensions". *International journal of bifurcation and chaos* 01, no. 04(1991): 745-772. doi:10.1142/s0218127491000555.

10. Doedel, Eusebius, Herbert B. Keller, and Jean Pierre Kernevez. "Numerical analysis and control of bifurcation problems (ii): bifurcation in infinite dimensions". *international journal of bifurcation and chaos* 01, no. 04 (1991): 745-772. doi:10.1142/s0218127491000555. [AUTO]

11. Doedel, Eusebius and Oldeman, Bart " AUTO-07p: Continuation and bifurcation software for ordinary differential equations, Concordia Univ, Version 0.9.1, 2012.

12. Coetzee, Etienne. *Dynamical Systems Toolbox* (version 3.1.0 (Beta)). MATLAB, 2014.

13. Guzzella, Lino, and Christopher H. Onder. *Introduction to Modeling and Control of Internal Combustion Engine Systems*. *Introduction to Modeling and Control of Internal Combustion Engine Systems*, 2010. https://doi.org/10.1007/978-3-642-10775-7

Contact Information

Shaun Smith
s.smith6@lboro.ac.uk

Acknowledgments

This research is funded through the EPSRC Centre for Doctoral Training in Embedded Intelligence, with industrial support from Jaguar Land Rover.